Evaluating the Potentiality of X-ray Tomography on the Quality Assessment of Grouted Soils

Alessandro Fraccica[1,2], Giovanni Spagnoli[3,4P(B)], Enrique Romero[1,5], and Marcos Arroyo[1,5]

1 Geomechanics Group, International Centre for Numerical Methods in Engineering,
UPC calle Gran Capità S/N, 08034 Barcelona, Spain
2 Italian Institute for Environmental Protection and Research, ISPRA, Via Brancati 48,
00144 Rome, Italy
3 MBCC Group, Dr. Albert Frank Str. 32, 83308 Trostberg, Germany
spagnoli_giovanni@yahoo.de, giovanni.spagnoli@dmt-group.com
4 DMT GmbH & Co. KG, Am TÜV 1, 45307 Essen, Germany
5 Department of Civil and Environmental Engineering, Universitat Politècnica de Catalunya,
calle Jordi Girona 1-3, 08034 Barcelona, Spain

Abstract. Grouting is a technique used to improve the engineering properties of soils and rocks. Grouting techniques are classified under different criteria: injection method used, type of grout material injected, typical application, and the sequence of construction. The best-known criterion is the mode of entrance or admission of grout into the soil or rock. It is possible to identify therefore several grouting techniques: compaction, fracture, jet/mixing and permeation. The function of penetration grouting is to reduce the permeability of the soil or rock and/or increase the strength and density. In order to avoid displacements or piston effects, permeation grouting shall be carried out at carefully controlled pressures and flow rates, using appropriate grouts. Several tests have been performed, with a laboratory injection device, on four soil mixtures with different permeability values (k_w values between 10_{-4} and 10_{-7} m/s) and the same void ratios, injected with a colloidal silica. Indirect tests (X-ray CT-scans) and destructive tests (unconfined compressive strength tests) were performed to assess the injection effectiveness and the grade of mechanical improvement achieved. The chosen binderwas able to penetrate in low permeable soils with k_w values of 10_{-7} m/s. Results are valuable for contractors and designers involved in the consolidation of soils where k_w values are known.

Keywords: X-ray CT-scan · Soil · Grouting · Unconventional binders

1 Introduction

In many geotechnical operations the construction of structures frequently requires improvement of the mechanical properties and behavior of soils by permeation grouting using either cementitious or chemical grouts (Christodoulou et al. 2009). Geotechnical contractors aim to extend the injectability range of grouts in soils with higher fine content. However, it is obvious that grout cannot penetrate all the voids (Cambefort 1977). Initial soil permeability is the primary guide to establishing the groutability of a soil mass. According to the U.S. Department of Transportation (1983) soils having permeabilities up to 10^{-5} m/s are easily groutable. Soils showing permeabilities up to 10_{-6} m/s are moderately groutable, being 10^{-6} m/s the limit of groutability according to Cambefort (1977), and soils with permeabilities above 10^{-7} m/s are considered ungroutable. Microfine cements and chemical grouts have been developed to grout soils which are otherwise ungroutable due to the gradation or fine content (Spagnoli 2021).Many novel technologies have been tested so far: microfine cements were developed in Japan in the 1970s and introduced to the USA in the 1980s, to be an alternative to chemical solution grouts by extending the application range of ordinary cement grouts in permeation grouting for ground improvement (Pantazopoulos et al. 2021). Resins such as epoxy (Anagnostopoulos and Hadjispyrou 2004) are used where high rapid gain of strength, high resistance to high groundwater flows and variable setting times are needed (Bruce et al. 1997). Colloidal silica is a new technology made by extracting alkali from sodium silicate with ion-exchange resin and tested both in laboratory and in real job sites (e.g. Gallagher et al. 2007; Spagnoli et al. 2022a; Salvatore et al. 2020). Generally, core drilling and in-situ (CPT, SPT,…) or laboratory (UCS, triaxial compressions) mechanical tests are conducted to verify the effective penetration of the binder into the soil. This phenomenological approach needs to be complemented by microscale analyses when the penetrability of new binders in low permeable soils (e.g. with water permeability of 10^{-6} m/s or less) needs to be studied and numerically modelled in the context of research and development. Indirect methods formicro-scale investigations, such as X-ray tomography, have been used in many geotechnical studies (Andò et al. 2013; Viggiani et al. 2015; Kabilan et al. 2016; Zhang et al., 2018; Fraccica 2019; González Blanco et al. 2020 among others) whereas they are less common for grouted soils (Takano et al. 2013; Bezuijen and Van Tol 2006; Pedrotti et al. 2020). Due to the above, the aim of this paper is to present results from X-ray tomography as a technique to verify the effectiveness of injecting low-viscosity binders into specimens with different water permeabilities and check the quality of the samples prepared and cured for UCS tests.

2 Materials and Methods

The soils used in this study are derived from four different mixtures of Holcim Sand (Spagnoli et al. 2022b; Fraccica et al. 2021) and Llobregat Silty Sand (Fraccica 2019) sieved at 0.425mm.The firstmaterial is a homogeneous siliceous sand,

while thematerial resulting from sieving is a silt of low plasticity. The latter was wetted at a water content w = 18% and subsequently re-sieved to obtain clay aggregates no larger than 2 mm. The mixtures of the two soils had final weight percentages of Holcim sand of 0%, 30%, 45% and 70%. The proportions of the two soils were designed to obtain specimens with saturated water permeability varying between 10^{-7} and 10^{-4} m/s and a similar dry density ($\rho_d \approx$ 1.57–1.58 Mg/m^3), obtained after static compaction. Soil samples were compacted in three layers and had always the same final size (h=150 mm,Φ =70 mm). The soil mixtures are presented in the Table 1.

Table 1 List of proportions, permeability and granulometry indexes of the soil mixtures investigated

Mixture water permeability, k_w (m/s)	% Holcim Sand (w/w)	% Llobregat Silty Sand (0.425mm) (w/w)	Soil grain size at 50% passing fraction, d_{50} (mm)	Soil grain size at 15% passing fraction, d_{15} (mm)
10-4 m/s	70	30	0.425	0.040
10-5 m/s	45	55	0.315	0.010
10-6 m/s	30	70	0.150	0.007
10-7 m/s	0	100	0.040	0.004

The binder used was a suspension (Colloidal Silica with 15% of silica (w/w)), with particles of mean size 1.5 · 10^{-5} mm (Wong et al. 2018). The specimens compacted in a stainless-steel container were first saturated with water and then injected with the different binders. In both cases, the fluids flowed from the bottom to the top, forced through a GDS that controlled the pressure and volume of water exiting its piston. In the case of binder injection, a water/binder interface was adopted (Fig. 1a), and the injection process lasted 45 min. Injection pressures were kept below one third of the vertical compaction stress at all times in order to avoid piston effects.

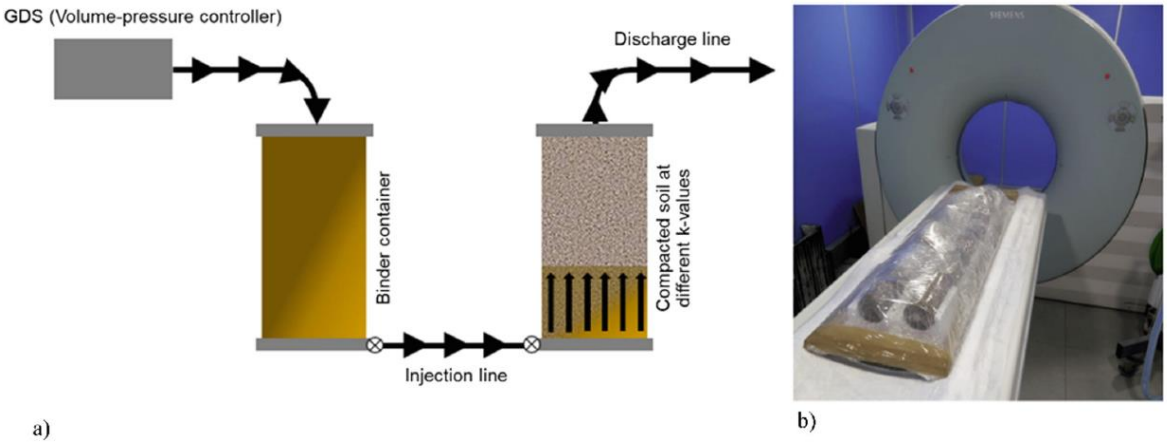

Fig. 1. a) Injection system b) X-ray tomograph and samples setup.

After extraction of the specimens from the containers and curing at relative humidity RH = 100% for 28 days, the quality of the injection was checked by X-ray tomography prior to UCS testing. Tomography was carried out with a medical scan (Siemens Somatom Spirit®), with an X-ray beam with average energy 130 keV and tube current 48 mA, resulting in image stacks with voxel size of 0.40 × 0.40 × 1.50 mm^3. Jointly with grouted and pure soil samples, and pure binder samples, four objects with known bulk density were scanned (Fig. 1b): two sand samples, one calcium carbonate powder sample and one crystal sphere. These known densities, as well as that of air at atmospheric pressure, were linked to the grey value that the respective objects had in the images, resulting in a good linear correlation (Fig. 2a). By means of this calibration, it was possible to evaluate the densities of the pure and injected soil samples in order to make a comparative analysis and thus distinguish the areas in which the binder might have deposited. As the size of the individual voxel in the X-ray images is much larger than that of the soil grains (e.g. at a ratio of 1:2000 in the case of the 100% silt specimen and 1:2 in the case of the 70% Holcim sand specimen, see d_{50} in Table 1), it is not possible to visually distinguish the latter from solidified binder aggregates. Soil and binder are therefore present, on average, within some voxels. Other voxels instead include soil grains and air particles in different proportions and are clearly identifiable as separate modes in the stack's grey value histogram (Fig. 2a).

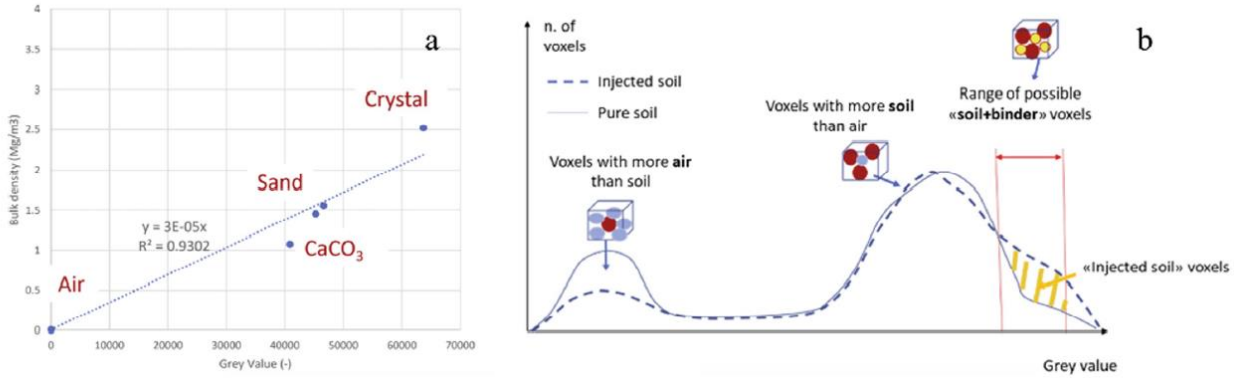

Fig. 2. a) Correlation between bulk density and grey value of calibration objects of known density and b) Comparison of grey value theoretical histograms of pure and injected soil.

This means that the grey value of one *injected soil* voxel will be a linear combination of the grey value of the pure binder and of the pure soil. This theory has been formalised by Luo et al. (2008) through the Eq. (1):

$$GV(x,y,z) = GV(x,y,z)_{solid}[1 - n(x,y,z)] + GV(x,y,z)_{water} n(x,y,z) S_{r,water} + GV(x,y,z)_{air} n(x,y,z) S_{r,air} \quad (1)$$

where *GV(x,y,z)* is the grey value of the soil at a given point of the 3Dimage, obtained as a linear combination of the grey values of soil grains (*solid*),water and air.Weighing factors are the soil porosity *n(x,y,z)* and the values of degree of saturation S_r of the fractions (air and water). In this study, Eq. (1) was adapted by replacing the water fraction with the binder one, and neglecting the air fraction (i.e. $S_{r,binder} = 1$, and $S_{r,air} = 0$). A range of GV_{binder} (average • } standard deviation of the grey value of the pure binder, assessed by X-ray tomography) was used instead of GV_{water} . The average porosity in the samples was $n = 0.407$. With this procedure it was possible to perform a segmentation in *ImageJ* (Schindelin et al. 2012) and thus isolate a range of *GV* of the *soil + binder* voxels (Fig. 2b). Within this range, the number of voxels of the injected specimen was subtracted from that of the pure soil specimen: in this way the voxels with the highest probability of containing the binder were isolated (Fig. 2b). Once isolated, *ImageJ* proceeded to count the specific voxels (in white in Fig. 3a) and hence to give their overall volume. The latter volume is the one of the *injected soil* voxels. The volume of the binder (*sub-voxel* level) present within the soil was inferred multiplying the volume of the *injected soil* voxels by the soil average porosity, assuming that pores are fully saturated by the Colloidal Silica. Using these two techniques, 3Dimages were produced to qualitatively observe the arrangement of the binder within the specimens. These techniques are complementary because one allows to compare soil bulk density before and after the injection while the other gives the possible 3D arrangement of the binder within the soil matrix.

3 Results and Discussion

The volume of binder within the soil specimen was calculated by *ImageJ* (Fig. 3a) from X-ray images and was verified by measurements of the GDS and the liquid released from the discharge line. The three measurements were in good correlation among them. The volume of the binder was normalised with respect to the whole volume of pores in the samples to infer the binder degree of saturation ($S_{r,binder} = V_{binder}/V_{pores}$ with average $V_{pores} = 235.2$ cm3) of the Colloidal Silica at the end of the curing period (Fig. 4). This ratio was correlated to the unconfined compressive strength observed in the respective sample, showing a significant linear trend.

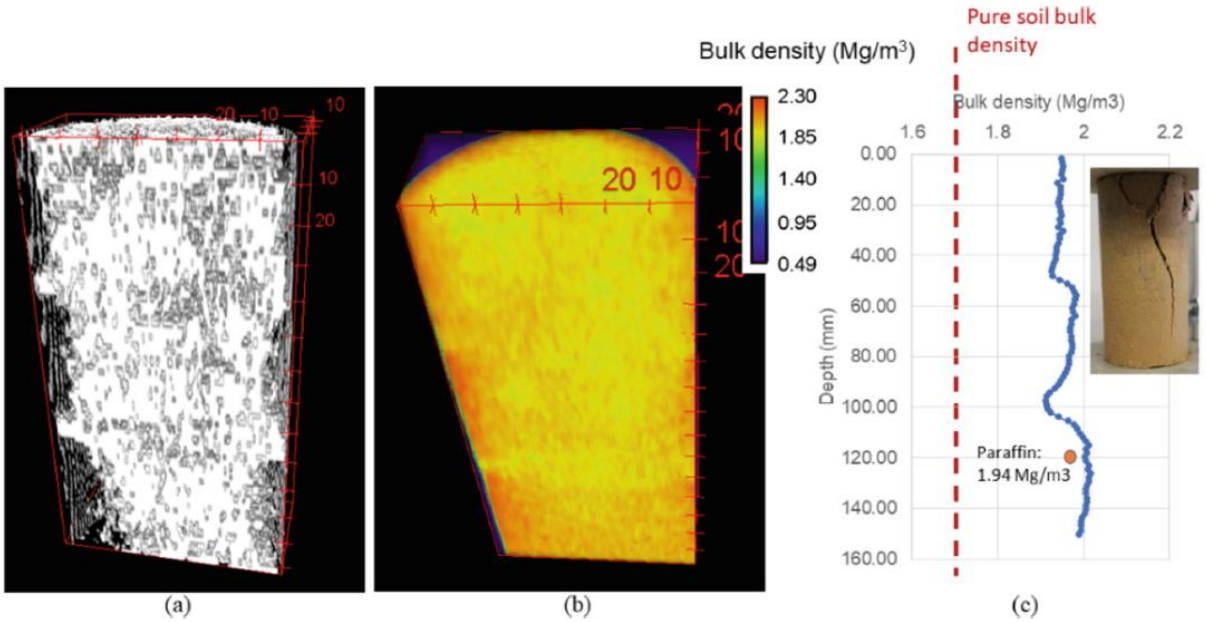

Fig. 3. Sample with initial water permeability of 10–5 m/s, after Colloidal Silica injection. a) isolation of voxels (white) including binders, b) bulk density 3D map and c) bulk density profile along sample height, with paraffin test check.

Generally, it was observed that as the permeability of the soil specimen increased, a greater volume of binder was able to penetrate the specimen. In the case that any test specimen contained a portion of soil that had not been injected, this was removed by spatula before the UCS test. Observing the results, a good correlation can be found between the strength of the grouted samples and their binder degree of saturation inferred by X-ray images (Fig. 4).

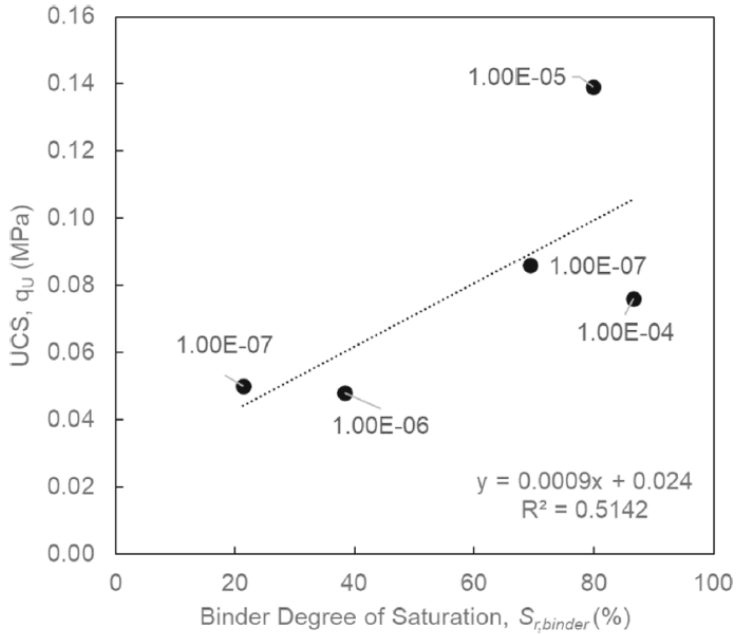

Fig. 4. Correlation between Unconfined Compressive Strength and binder degree of saturation. As-compacted water permeability indicated as label.

4 Conclusions

The preliminary results observed in this study are promising in view of the use of X-rays as a non-destructive technique for the quality control of soil samples injected with binders. Two complementary analyses can be carried out when X-ray images of un-grouted and grouted soils are available, apart from calibration objects with known density. Full 3D bulk density maps of the grouted soils can be easily reconstructed and mathematical operations at the *sub-voxel* level can produce good results in assessing the volume of binder injected into the soil. The grouted specimens generally showed higher bulk densities than the respective untreated specimens.As expected, sampleswith higher permeabilities showed higher binder degree of saturation and strength. Even specimens prepared entirely with sieved Llobregat silty sand and

with a permeability $k_w = 10^{-7}$ m/s were successfully injected, with a Colloidal Silica saturation degree between 20% and 68% and with a relatively good unconfined compressive strength.

Acknowledgements. The authors wish to thank Master Builders Solutions by MBCC Group for the permission granted to publish these results.

References

Anagnostopoulos, C., Hadjispyrou, S.: Laboratory study of an epoxy resin grouted sand. Proc. Inst. Civil Eng. Ground Improv. **8**(1), 39–45 (2004). https://doi.org/10.1680/grim.2004.8.1.39

Andò, E., Viggiani, G., Hall, S.A., Desrues, J.: Experimental micro-mechanics of granular media studied by x-ray tomography: recent results and challenges. Géotech. Lett. **3**(3), 142–146 (2013). https://doi.org/10.1680/geolett.13.00036

Bezuijen, A., Van Tol, A.F.: X-ray tomography in compensation grouting research: shape and density of injected grout. In: Advances in X-ray Tomography for Geomaterials, pp. 355–363. Wiley (2006). https://doi.org/10.1002/9780470612187.ch37

Bruce, D.A., Littlejohn, G.A., Naudts, A.M.C.: Grouting materials for ground treatment: a practitioner's guide. In: Vipulanandan, C. (ed.) Grouting: Compaction, Remediation and Testing, no. 66. American Society of Civil Engineers. GSP Geotechnical Special Publication (GSP), New York (1997)

Cambefort, H.: The principles and applications of grouting. Q. J. Eng. Geol. Hydrogeol. **10**, 57–95 (1977). https://doi.org/10.1144/GSL.QJEG.1977.010.02.01

Christodoulou, D.N., Droudakis, A.I., Pantazopoulos, I.A., Markou, I.N., Atmatzidis, D.K.: Groutability and effectiveness of microfine cement grouts. In: Proceedings of the 17th International Conference on Soil Mechanics and Geotechnical Engineering, vols. 1, 2, 3 and 4, pp. 2232–2235. IOS Press (2009)

Fraccica, A.: Experimental study and numerical modelling of soil-roots hydro-mechanical interactions.Ph.D. thesis, Université de Montpellier (UM), France and Universitat Politécnica de Catalunya (UPC), Spain (2019)

Fraccica,A., Spagnoli, G.,Romero,E., Arroyo, M.,Gómez, R.:Exploring the mechanical response of low-carbon soil improvement mixtures. Can. Geotech. J. (2021). https://doi.org/10.1139/cgj-2021-0087

Gallagher, P.M., Conlee, C.T., Rollins, K.M.: Full-scale field testing of colloidal silica grouting for mitigation of liquefaction risk. J. Geotech. Geoenviron. Eng. **133**, 186–196 (2007). https://doi.org/10.1061/(ASCE)1090-0241(2007)133:2(186)

González Blanco, L., Romero Morales, E.E., Marschall, P.: Gas transport in granular compacted bentonite: coupled hydro-mechanical interactions andmicrostructural features. In: Proceedings of EUNSAT 2020, 19–21 October 2020, Lisbon, Portugal E3S Web of Conferences, vol. 195, p. 04008-1. EDP Sciences (2020). https://doi.org/10.1051/e3sconf/202019504008

Kabilan, S., et al.: Numerical simulation of permeability change in wellbore cement fractures after geomechanical stress and geochemical reactions using x-ray computed tomography imaging. Environ. Sci. Technol. **50**(12), 6180–6188 (2016). https://doi.org/10.1021/acs.est.6b00159

Luo, L., Lin, H., Hallek, P.: Quantifying soil structure and preferential flow in intact soil using x-ray computed tomography. Soil Sci. Soc. Am. J. **72**(4), 1058–1069 (2008). https://doi.org/10.2136/sssaj2007.0179

Pantazopoulos, I.A., Markou, I.N., Atmatzidis, D.K.: Performance of microfine cement grouted sands under quick loading conditions. Int. J. Geosynth. Ground Eng. **7**(1), 1–17 (2021). https://doi.org/10.1007/s40891-021-00255-0

Pedrotti, M., Wong, C., El Mountassir, G., Renshaw, J.C., Lunn, R.J.: Desiccation behaviour of colloidal silica grouted sand: a new material for the creation of near surface hydraulic barriers. Eng. Geol. **270**, 105579 (2020). https://doi.org/10.1016/j.enggeo.2020.105579

Salvatore, E., Modoni, G., Mascolo, M.C., Grassi, D., Spagnoli, G.: Experimental evidences on the effectiveness and applicability of colloidal nanosilica grouting for liquefaction mitigation. J. Geotech. Geoenviron. Eng. **146**, 04020108 (2020). https://doi.org/10.1061/(ASCE)GT.1943-5606.0002346

Schindelin, J., et al.: Fiji: an open-source platform for biological-image analysis. Nat. Methods **9**, 676–682 (2012). https://doi.org/10.1038/nmeth.2019

Spagnoli, G.: A review of soil improvement with non-conventional grouts. Int. J. Geotech. Eng. **15**(3), 273–287 (2021). https://doi.org/10.1080/19386362.2018.1484603

Spagnoli, G., Chittenden, N., Grassi, D., Joaquin Cortez, J.: Case histories on the applications of colloidal silica for permeation grouting. In: DFI-EFFC International Conference on Deep Foundations andGround Improvement: Smart Construction for the Future, pp. 202–211 (2022a)

Spagnoli, G., Romero, E., Fraccica, A., Arroyo, M., Gómez, R.: The effect of curing conditions on the hydro-mechanical properties of a metakaolin-based soilcrete. Géotechnique **72**(5), 455–469 (2022b). https://doi.org/10.1680/jgeot.20.P.259